scientific reports

Check for updates

OPEN

Macromolecular protein crystallisation with biotemplate of live cells

Mubai Sun[1], Huaiyu Yang[2]✉, Xinyu Miao[1], Weixian Wang[3] & Jinghui Wang[1]✉

Macromolecular protein crystallisation was one of the potential tools to accelerate the biomanufacturing of biopharmaceuticals. In this work, it was the first time to investigate the roles of biotemplates, Saccharomyces cerevisiae live cells, in the crystallisation processes of lysozyme, with different concentrations from 20 to 2.5 mg/mL lysozyme and different concentrations from 0 to 5.0×10^7 (cfu/mL) Saccharomyces cerevisiae cells, during a period of 96 h. During the crystallisation period, the nucleation possibility in droplets, crystal numbers, and cell growth and cell density were observed and analysed. The results indicated the strong interaction between the lysozyme molecules and the cell wall of the S. cerevisiae, proved by the crystallization of lysozyme with fluorescent labels. The biotemplates demonstrated positive influence or negative influence on the nucleation, i.e. shorter or longer induction time, dependent on the concentrations of the lysozyme and the S. cerevisiae cells, and ratios between them. In the biomanufacturing process, target proteins were various cells were commonly mixed with various cells, and this work provides novel insights of new design and application of live cells as biotemplates for purification of macromolecules.

Therapeutic proteins provide effective treatments to a wide range of medical conditions and their demands have grown rapidly over the past two decades. The global sale of mAb products almost doubled from 2008 to 2013, reaching nearly $75 billion, and is expected to increase faster in this decade[1]. The purification of therapeutic proteins is very expensive, due to the high cost of the chromatography method[2] for recovering the resin and scaling up[3,4], as well as a large footprint for the product and environment[5,6]. Crystallisation has been a potential purification and isolation method[7–11], which widely used in small organic molecular pharmaceutical purification. Macromolecular protein crystallisation[12] has the potential to significantly simplify the downstream biomanufacturing process, achieving a significant waste reduction. Therapeutic proteins in the crystalline form have multiple advantages over their solution counterpart including higher stability[13–15]. However, due to the difficulty of large and flexible proteins forming highly ordered structure[16,17], nucleation and crystal growth are still challenging in industrial applications. More research on protein crystallisation was reported and with attempts to accelerate the nucleation and as the purification process is limited by the crystallisation time[18]. Different solid templates (i.e. heterogeneous particles and solid surfaces) have been investigated to improve the protein crystallisation efficiency[19–26] and shorten the crystallisation process. Protein crystallisation becomes more difficult due to the presence of biological impurities such as cell debris, host cell protein, DNA and virus, among which host cell protein normally has the highest concentration and hence poses the greatest hindrance to the success of crystallisation[27]. In order to better connect the upstream bioprocess and downstream bioprocess, it is critical to understand the influence of the impurities such as cells on the crystallisation process.

Saccharomyces cerevisiae (S. cerevisiae) with a short growth cycle and strong fermentation capacity, is widely used in the large-scale production of wine, foods, chemical products and pharmaceuticals[28–30]. Its diameter is 5–10 μm, and the cells are spherical or oval. The cell wall of yeast, for maintaining cell morphology and intercellular recognition, including 30% dry weight of mannan, 30% of β-Dextran, 20% of glycoprotein and chitin, and others[31]. Mannan has a three-dimensional spiral structure in space, and it also has a variety of physiological functions such as cell recognition and control of cell wall pore size. Mannan is chemically stable, with a relatively stable pH between 2.5 and 8.0[32,33]. Lysozyme can act on the β-1,4 bond between N-acetylmuramic acid and N-acetylglucosamine in the peptide polysaccharide molecule, which destroys the cell wall of bacteria, losing its

[1]Agricultural Products Processing Research Institute, Jilin Academy of Agricultural Science, Changchun 130124, Jilin, China. [2]Department of Chemical Engineering, Loughborough University, Leicestershire LE113TU, UK. [3]School of Materials and Chemistry, University of Shanghai for Science and Technology, Shanghai 200093, China. ✉email: h.yang3@lboro.ac.uk; wjhjaas@cjaas.com

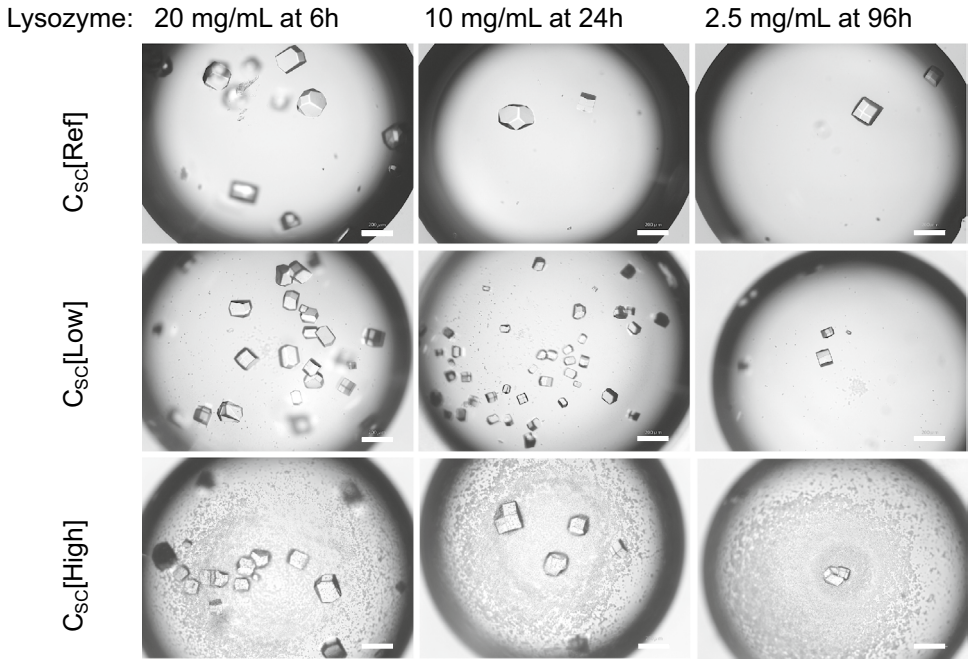

Figure 1. Microscope images of some droplets with the C_{Lys} of 20, 10 and 2.5 mg/mL and with three different concentrations of biotemplates. Scale bars are 200 μm.

protective effect on cells, and finally makes bacteria dissolve and die[34]. However, lysozyme has limited impact on the cell wall lysis of the S. cerevisiae, due to the lack of lysozyme sites in its cell wall[35,36].

To the best knowledge of the authors, the current study is the first to apply the biotemplates, live-cell templates, on protein crystallisation, this research will fill the technology gap by demonstrating the feasibility of yeast cells, S. cerevisiae, as a heterogeneous nucleant to promote the crystallisation of a model protein, lysozyme. The work also demonstrated the crystallisation technology has the ability to isolate protein in the complex solution environment with various concentrations of the live cells. The knowledge provided in this study can be transformed into future applications of biotemplate design for bioseparation and purification of therapeutic proteins or other macromolecules.

Results

Figure 1 shows the examples of formation of protein crystals inside droplets with and without biotemplates at various time dependent on the concentration of the protein. The droplets with biotemplates at C_{SC}[Low] of the biotemplates had much more crystals, and the crystals were obviously smaller, as well as more uniformed, than the crystals obtained in the droplets with biotemplates at C_{SC}[High]. It is obvious that plenty of S. cerevisiae cells were observed in the droplets with biotemplates at C_{SC}[High], much fewer S. cerevisiae was observed in the droplets with biotemplates at C_{SC}[Low]. The crystals had light agglomerations with a lower concentration of biotemplates, but there was no agglomeration observed in the droplets without and with a high concentration of S. cerevisiae. There was no obvious trend in the change of the crystal shape in the droplets with different concentrations of the biotemplates.

Figure 2 shows the accumulative possibility of the nucleation, i.e. the percentage of droplets with at least one crystal inside. The longer crystallisation time was, the nucleation occurred in more droplets at all the conditions. With the same concentration of S. cerevisiae biotemplates in the solution, the crystallisation time decreased with an increase in the concentration of lysozyme. The nucleation percentage curves show consistent trends, as the higher concentration of the lysozyme in the solution was, the higher driving force (supersaturation) for the nucleation in the droplets could become. When the C_{Lys} was 2.5 mg/mL, the nucleation time increased dramatically, only 20% of droplets nucleated in 60 h crystallisation time with or without biotemplates. When the C_{Lys} increased to 7.5 mg/mL and above, nucleation occurred in more than 50% of droplets in 20 h, and there was nucleation in less than 4 h in all the droplets with the C_{Lys} of 20 mg/mL. However, it is noted that with different concentrations of biotemplates, the crystallisation percentages were different in the droplet with the same C_{Lys}. Figure 3 shows the percentage change of the droplets with nucleation in 0–24 h crystallisation time. When the C_{Lys} was 2.5 mg/mL, no nucleation was observed in 24 h, and with an increase in the C_{Lys}, more droplets with crystals were observed, and there were crystals in almost all of the droplets with C_{Lys} above 7.5 mg/mL at 24 h.

It is obvious that the S. cerevisiae as biotemplate had strong influences on the nucleation and crystallisation process, and positive or negative influences were dependent on the concentrations of the lysozyme and the biotemplates. The possibility of the nucleation at 24 h follow the order in the droplets at an equal C_{Lys} of 10 or 20 mg/mL: with C_{SC}[Low] > with C_{SC}[High] > with C_{SC}[Ref], and at an equal C_{Lys} of 5 or 7.5 mg/mL, the order changed to: with C_{SC}[Low] > with C_{SC}[Ref] > with C_{SC}[High]. At 2.5 mg/mL, the order of the nucleation possibility

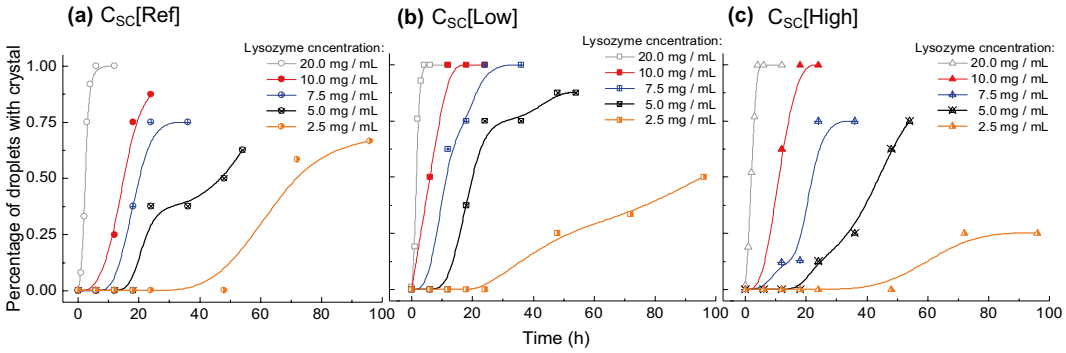

Figure 2. Percentage of droplets with crystals during crystallisation time of 96 h in the solution of 2.5–20.0 mg/mL lysozyme and without biotemplates (**a**), with a low concentration of biotemplates (**b**) and high concentration of biotemplates (**c**).

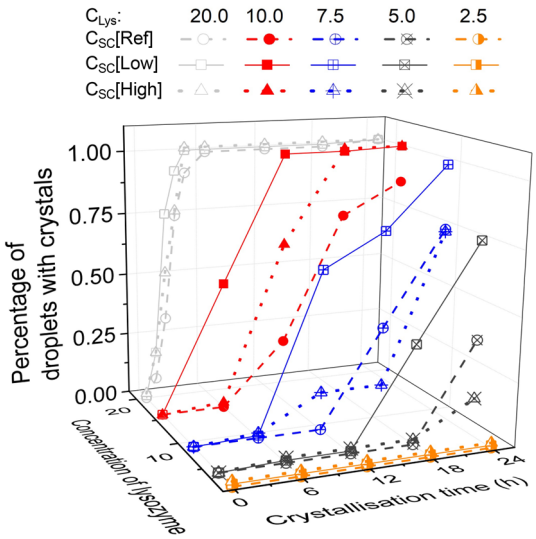

Figure 3. Percentage of droplets with crystals during crystallisation time of 24 h in the solutions with 2.5–20.0 mg/mL lysozyme, and without and with a low and high concentration of biotemplates.

in the droplets became: with C_{SC}[Ref] > with C_{SC}[Low] > with C_{SC}[High], shown in Fig. 2. At the high C_{Lys}, S. cerevisiae as biotemplates increased the nucleation rate, at the middle range of the C_{Lys}, only a low concentration of S. cerevisiae prompted the nucleation, and the high concentration of S. cerevisiae hindered the nucleation compared with the droplets without S. cerevisiae. The trend was consistent that with the C_{Lys} decreased to 2.5 mg/mL, both high and low concentrations of S. cerevisiae slowed the nucleation rates. The trend indicates that the biotemplates would accelerate the nucleation possibility, but too many templates would lead to an opposite effect. The results were also in the agreement with the median induction time shown in Fig. 4. The induction times were all shorter with biotemplates in the droplets, except in the condition with the C_{Lys} at 2.5 mg/mL. The high concentration of the biotemplates tended to be of less effect or negative effect in the droplets with lower C_{Lys}. The overall median induction time increased with a decrease in the C_{Lys} as expected.

The low concentration of biotemplates did not only facilitate the nucleation, but also boosted the quantity of the crystals in the droplets. Due to different time scales for different crystallisation conditions, three groups at different C_{Lys} were compared. At C_{Lys} of 20 mg/mL, the average number of crystals in each droplet were all over one hundred in less than 8 h, and the differences between the droplets with different concentrations of biotemplates were not obviously observed. Figure 4 shows the other two groups. In the lysozyme concentration range of 10–5 mg/mL, at 24 h the average number without biotemplates and with a high concentration of template were all below 10, but the number of crystals with a low concentration of the bio-templates were much higher, with above 8 times differences. At very low C_{Lys}, there was few droplets with crystals at 24 h, and at 96 h, there were only a few crystals in each droplet without big differences for droplets with different concentrations of biotemplates. In all the conditions, the average numbers of crystals in the droplets with biotemplates at C_{SC}[Low] were much higher than the droplets without biotemplates. The average numbers of crystals in the droplets with

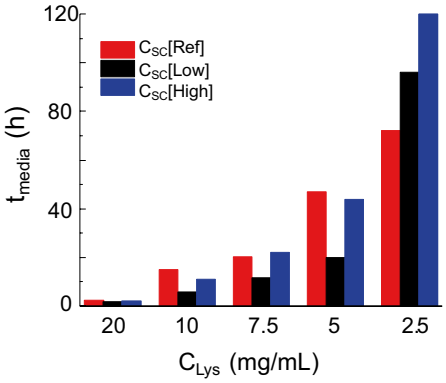

Figure 4. Median induction time extrapolated from Fig. 2 in the droplets with the C_{Lys} of 2.5–20 mg/mL and three different concentrations of the biotemplates.

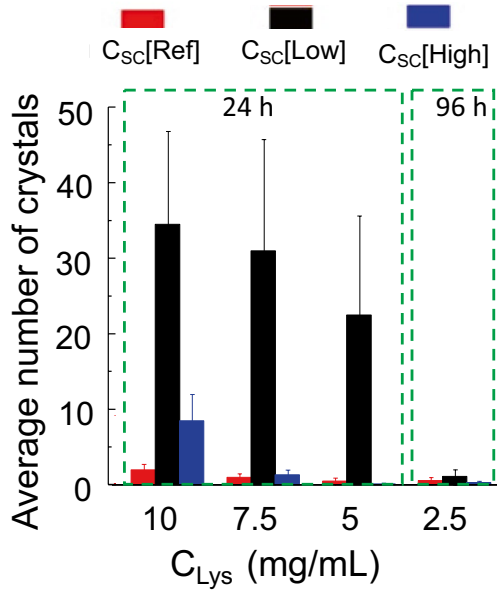

Figure 5. Average numbers of crystals obtained in each droplet at the C_{Lys} of 10, 7.5 and 5 mg/mL at 24 h, and at C_{Lys} of 2.5 mg/mL at 96 h.

biteplates at C_{SC}[Low] were higher than those without biotemplates, but the order tended to be reversed in the droplets with low C_{Lys} (Fig. 5).

To further understand the interactions of the biotemplates with lysozyme protein, the solutions with S. cerevisiae at C_{SC}[Low] or C_{SC}[High] were pre-mixed with the protein solution of the C_{Lys} of 5–10 mg/mL for 2 and 4 h before adding precipitation solution into the droplet. The percentage of droplets with crystals inside were compared, shown in Fig. 6 at 12 h after mixing with precipitation solution. The droplets with protein solution premixed with bio-templates had a slower nucleation rate than the droplets without premixing of the biotemplates in most of the cases. The stronger negative influence on nucleation was observed in the droplets with low C_{Lys}, and in the droplets with C_{Lys} of 5.0 mg/mL and with biotemplates at C_{SC}[High], only less than 70% of droplets occurred nucleation compared with the droplets without premixing of the bio-templates at equal crystallisation condition. In the droplets with C_{Lys} of 7.5 mg/mL and with the bio-templates premixed, overall less than 20% of the droplets occurred nucleation compared with the droplets without the premixing of the biotemplates at equal crystallisation condition. There was no obvious influence of the pre-mixing of the biotemplates in the droplets of C_{Lys} at 10 mg/mL, and the premixed biotemplates at C_{SC}[High] tended to have stronger negative influence than those at C_{SC}[Low]. There was no obvious trend in comparison between the droplets with the premixed biotemplates for 2 h and 4 h, indicating the interactions between the lysozyme and the biotemplates were established in a short period.

Figure 7 shows that there was no obvious change in the morphology of the S. cerevisiae in the buffer solution, the lysozyme solution or the crystallisation solution (lysozyme solution mixed with sodium chloride solution).

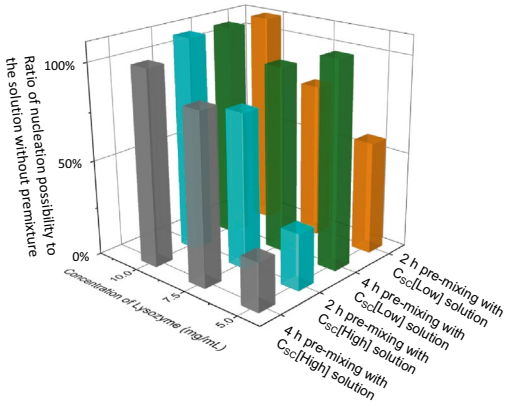

Figure 6. Ratios of nucleation possibility between the droplets with C_{Lys} at 5–10 mg/mL and with premixed bio-templates at C_{SC}[Low] or C_{SC}[High] for 2 h and 4 h to the droplets with equal condition (no premixing).

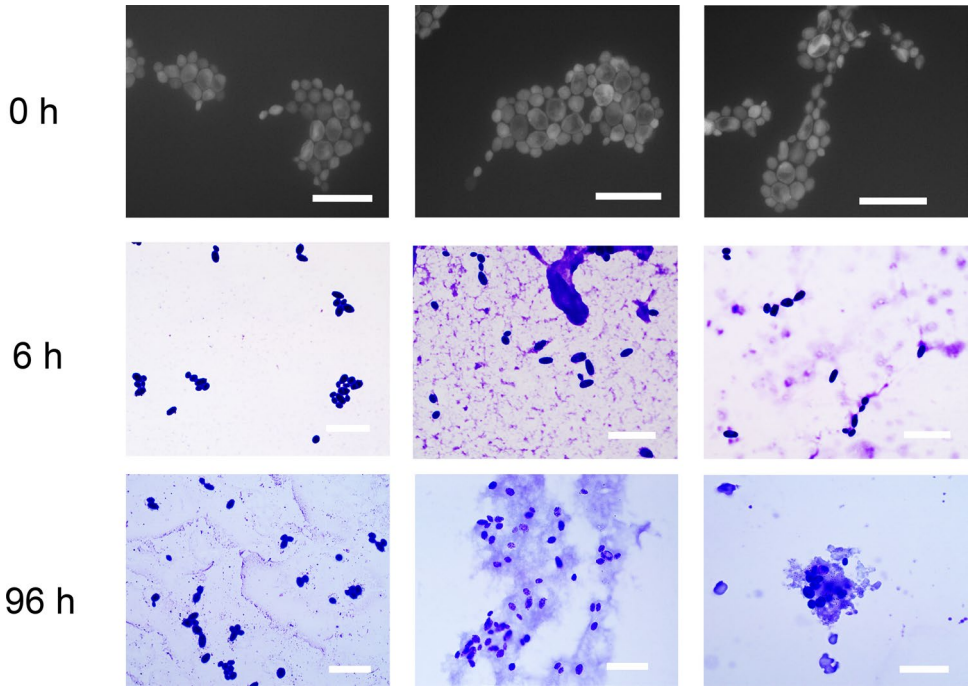

Figure 7. Cell culture of S. cerevisiae in the buffer solution, the lysozyme solution and the crystallisation solution (protein solution mixed with precipitation solution) from left to right columns, respectively, with scale bar of 20 μm.

Under the fluorescence microscope, there was no obvious fragmentation of the S. cerevisiae observed during 96 h in two kinds of solutions with the lysozyme, indicating that lysozyme did not lead to the lysis of the S. cerevisiae, which was in agreement with the literatures[35,36]. Most S. cerevisiae survived with lysozyme in the solution, and maintained its morphology during the crystallisation, shown in SEM images of Fig. 8. It was reported that S. cerevisiae is capable to overcome stress and survive with good tolerance to ethanol, high salt concentrations and oxidative damage[37,38].

The results of the spread plate method in Table 1 show that the density of S. cerevisiae cells in the three solutions all increased, but increase rates were much slower than the growth rate in culture solutions with suitable conditions. It was reported that in a suitable concentration of glucose, yeast cells grew exponentially by fermentation and the number of cells would be double in 90 min[39], leading to a 16 folds increase in 6 h. In this work, at 6 h, S. cerevisiae increased only 4–5 folds in the solution without lysozyme and increased less than 2 folds in two solutions with lysozyme. At 96 h, the densities of S. cerevisiae all further increased, about 7 folds and 4–5 folds in the solutions with lysozyme and without lysozyme, respectively. It is noticed that with lysozyme the density of S. cerevisiae was much lower than the solution without lysozyme, showing the interactions between

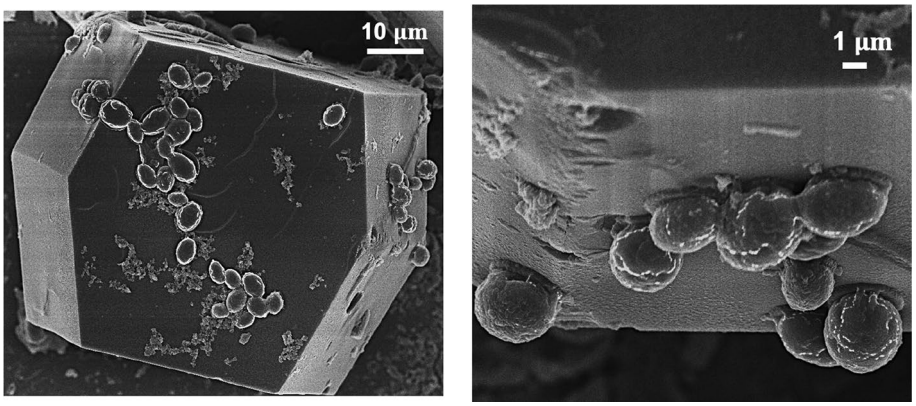

Figure 8. SEM images of S. cerevisiae and lysozyme crystal from hanging-drop experiments with C_{SC}[Low] biotemplates and 20 mg/mL lysozyme.

Solution	Concentration of S. cerevisiae (10^7 cfu/mL)		
	In buffer solution	In lysozyme	In lysozyme + salt
0 h	1.0	1.0	1.0
6 h	4.5	1.6	1.4
96 h	6.9	4.6	4.4

Table 1. The concentrations of S. cerevisiae in the buffer solution, the lysozyme solution and the crystallisation solution (lysozyme with salt).

the lysozyme and the cells, and in the solution with lysozyme without salt was slightly higher than the solution with lysozyme and salt.

Discussion

The interactions between the surface/cell wall of S. cerevisiae with the lysozyme affected the crystallisation processes. As heterogeneous surfaces would accelerate the nucleation by decreasing the nucleation free energy[40,41]. Compositions of cell wall of the S. cerevisiae, such as mannoproteins, polysaccharide complexes, and glucan network could be possible heterogeneous nucleants for the lysozyme crystallisation. Some nanoparticles can be encapsulated inside lysozyme crystal[42,43], but it is not possible to trap S. cerevisiae due to its big size, and, therefore, all the biotemplates should be outside the crystal or on the surface of the crystal, shown in Fig. 8. The observation of the crystallisation process, the cell culture process (Fig. 7), the cell density (Table 1) and the SEM images (Fig. 8) supported that the lysozyme did not lead to the lysis of the S. cerevisiae cells, but obviously hindered the growth and proliferation of the cells, indicating strong interactions between the cell wall and the lysozyme molecules. These interactions were also proved by the images of the crystallisation of the fluorescent lysozyme in Fig. 9. At the initial stage, after mixing the lysozyme with biotemplates, the fluorescent lysozyme fast attached on the cells, making all cells fluorescent, and there were also aggregations of lysozyme around cells, shown in Fig. 9C. At later stage, during and after nucleation, more aggregations were observed around the cells. The interactions between protein and protein were reported in other systems that aggregations of fluorescent-tag proteins were tracked under the fluorescence microscope[44,45]. The adsorption on the cell surface or the aggregation can result from electrostatic interactions[44,46,47], as one of most factors to influence the folding and binding of the protein, and the rate of protein–protein association, which also supported by the simulation with the docking methods[48]. Therefore, these interactions could result in adsorption or accumulation of lysozyme molecules on the cell surface, contributing to the promotion of the aggregation process during the pre-nucleation process and crystal growth process. Similar phenomena were reported in other systems, such as the formation of crystals of chernikovite salts on the surface of S. cerevisiae[49], and biosorption of copper[50] ions on the cell surface of S. cerevisiae. It is noted that only edge of the crystals of the tagged lysozyme appears fluorescent in Fig. 9 (see crystals in the whole droplet in supporting information), indicating the crystalline lysozyme disabled the fluorescent tag but the lysozyme starting to grow on the crystal surface still maintain fluorescent.

Most of the crystallisation experiments were completed at 96 h, during which period the density of S. cerevisiae increased less than 5 folds. The increase in the number of the biotemplates would influence heterogeneous nucleation, due to an increase in heterogeneous surface areas in the crystallisation solution. This can be one of the explanations of the trend shown in Fig. 6, higher nucleation possibility in the droplets with biotemplates premixed in the lysozyme solution. However, compared with two concentrations of the biotemplates between C_{SC}[Low] and C_{SC}[High] (which was of 100 times difference), the influences of changes in S. cerevisiae cell number were

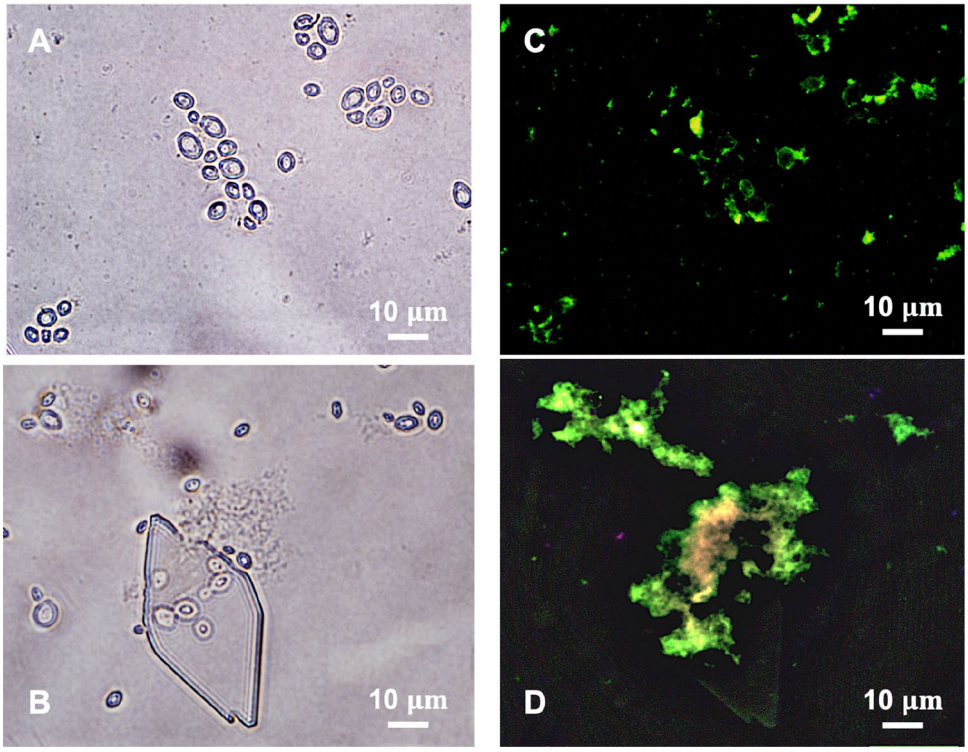

Figure 9. Optical microscope images of the fluorescent lysozyme before nucleation (**A**) and after nucleation (**B**), and corresponding fluorescence microscope images (**B**) and (**D**).

very limited. Therefore, the differences in induction time and crystals formation in the droplets, shown in Figs. 4 and 5, were mainly resulted from the initial concentration of the biotemplates in the crystallisation solution.

There were positive influences on the nucleation and crystal growth in the crystallisation solution of all the lysozyme concentrations, except 2.5 mg/mL, with biotemplates at both C_{SC}[Low] and C_{SC}[High]. However, a further large increase in the concentration of the biotemplates (at concentrations from C_{SC}[Low] to C_{SC}[High]) led less positive influences, i.e. the slower nucleation rates with the biotemplates at C_{SC}[High] than with the biotemplates at C_{SC}[Low]. Moreover, the ratio between the concentrations of the cells and the lysozyme would also determine the influence on the nucleation process, as negative influences were observed in the crystallisation solution of very low lysozyme concentration at 2.5 mg/mL with biotemplates at both low and high concentrations. The higher ratio between the concentration of the biotemplates to the lysozyme, the weaker the positive influence of biotemplates tended to be, turning into negative influences at very high ratios. It is noticed that the influences on the crystallisation process were not linear correlated to the ratio between concentrations of biotemplates and lysozymes. The possible reason can be that a large number of the S. cerevisiae would attract huge amount of the lysozyme molecules, diluting or hindering the formation of aggregations which could result in relatively low concentrations of lysozyme near or attach on the cell surface of each cell. Therefore, the high ratio between the number of biotemplates to the lysozyme molecules lead to the decrease in the driving force of the nucleation, hindering the crystallisation processes.

Conclusions

Various protein crystallisation processes with biotemplates of live cells were first time observed, proved to be contributed by the interactions between cell walls and lysozyme. The interactions were observed by the fluorescence lysozyme attached on the cell walls and aggregated around cells. The biotemplates of S. cerevisiae at low concentrations could facilitate the nucleation, with more droplets having crystals inside during the same period, and crystal growth of lysozyme, with the formation of more crystals. With the lysozyme in the solution, the cells would still grow without lysis but the density of the cells only slowly increased, indicating strong interactions between the lysozyme and the cell wall of S. cerevisiae. Protein molecules adhered on the cell wall of S. cerevisiae and aggregated around, and then the cell wall as heterogeneous surface decreased the nucleation free energy, leading to positive influences on the nucleation. These positive influences became weaker with a decrease in the concentration of lysozyme or a large increase in the concentration of biotemplates. With much lower ratios between concentration of the lysozyme to the biotemplates, the nucleation was hindered with a longer induction time. The crystal shape was not obviously influenced by the biotemplates at both high and low concentrations, but with low concentration of the biotemplates, there were always times more crystals formed in the droplets with more uniform size distributions.

C_{SC} (cfu/mL)	C_{NaCl} (mg/mL)	C_{Lys} (mg/mL)	Observation interval (h)	Total time (h)
C_{SC} [Ref]: 0.0 ($\pm 5\times10^5$)	80	2.5	6–24	96
C_{SC} [Low]: 5.0×10^4 ($\pm 5\times10^5$)		5.0	6–12	48
C_{SC} [High]: 5.0×10^6 ($\pm 5\times10^7$)		7.5	6–12	36
		10.0	6	24
		20.0	1	8

Table 2. Experimental conditions of the crystallisation with and without biotemplates. C_{SC} concentration of S. cerevisiae, C_{NaCl} concentration of sodium chloride, C_{Lys} concentration of lysozyme.

Materials and methods

Materials. Lysozyme (≥ 90%) was purchased from Sigma Aldrich (Gillingham, UK); FITC-labelled fluorescent lysozyme (> 90%) was purchased in Ruixi Biology); Chinasodium chloride, acetic acid glacial (> 99.7%) was purchased from Beijing Chemical Works (Beijing, China); sodium acetate (> 99.7%) was purchased from Xilong Scientific (Guangdong, China). Surfactant-free cellulose acetate membrane filter (0.22 μm) was purchased from Green Mall (Jiangsu, China). FDA/PI staining kits were purchased from BestBio (Shanghai, China). De-ionised water was used, and all chemicals were used as received without further purification.

Biotemplates preparation. S. cerevisiae was activated with LB medium, placed in a constant temperature incubator at 20 °C ± 0.2 °C, and cultured at 140 r/min for 0–96 h. The activated cell culture solution was diluted in sodium chloride solutions with different ccentrations of S. cerevisiae to prepare the precipitation solution used in protein crystallisation. The activated cell culture solution was diluted in buffer solution (0.14 M sodium acetate), lysozyme solution (10 mg/mL) and crystallisation solution (10 mg/mL lysozyme with 80 mg/mL NaCl). The number of S. cerevisiae cells were determined by the spread plate technique. The Gram staining method was used to observe the status of S. cerevisiae, and the cells of S. cerevisiae were observed under the microscope (Olympus DP71 Japan). The FDA/PI staining kit was used to perform fluorescent staining on S. cerevisiae cells, and the staining results were observed under the microscope (Olympus DP71, Japan).

Protein crystallisation. The sodium acetate buffer (0.14 M) was prepared by dissolving anhydrous sodium acetate in de-ionised water and followed by the addition of acetic acid to adjust the pH to 4.2. The sodium acetate buffer was filtered through a 0.22 μm filter. The preparation of protein solution was done by dissolving the protein (lysozyme, BSA or mixture) in the sodium acetate buffer. For example, to prepare a lysozyme solution with a target concentration of 20 mg/mL, lysozyme (20 mg) was dissolved in sodium acetate buffer (1 mL). Other solutions with concentrations of lysozyme from 10.0 to 2.5 mg/mL were prepared by dissolving corresponding amounts of lysozyme. Once lysozyme was fully dissolved, the solution was filtered through a 0.22 μm filter. Protein crystallization experiments were conducted using a conventional hanging-drop vapor diffusion technique. Crystallization drops were made by mixing 1.0 μL of protein solution and an equal volume of precipitation solution (80 mg/mL sodium chloride), with three different concentrations ($0–5\times10^6$ cfu/mL) of the S. cerevisiae, shown in Table 2. The final hanging drops of the mixture (2 μL) were sealed with a reservoir of sodium chloride solution (80 mg/mL), which were placed in the incubator at 20 °C ± 0.2 °C. In each crystallisation condition, 30–50 droplets were observed during the crystallization in the hanging droplets under a microscope (Olympus DP71) with time intervals between 1 and 24 h, dependent on the experimental conditions. To observe the aggregation of lysozyme during the crystallisation, hanging droplet experiments with fluorescent lysozyme at 20 mg/mL with low concentration of S. cerevisiae was performed as describe above, placing in the dark room for 4 h, then droplets were observed under an optical microscope (Olympus DP71) and fluorescence microscope (Olympus, Japan), with the green fluorescence at 495 nm.

Samples for SEM. The solution of hanging droplets with lysozyme crystals was contacted the silicon wafer carrier, then the filter paper was used to absorb the solution on the silicon wafer. The sample on the silicon wafer was air-dried and sprayed with Pt film, then was observed by scanning electron microscope (SEM, JEOL, Japan) .

Received: 12 October 2021; Accepted: 28 January 2022
Published online: 22 February 2022

References

1. Ecker, D. M., Jones, S. D. & Levine, H. L. The therapeutic monoclonal antibody market. *MAbs* **7**, 9–14 (2015).
2. Zou, X., Zhang, Q., Lu, H., Lin, D. & Yao, S. Development of a hybrid biomimetic ligand with high selectivity and mild elution for antibody purification. *Chem. Eng. J.* **368**, 678–686 (2019).
3. Shukla, A. A., Wolfe, L. S., Mostafa, S. S. & Norman, C. Evolving trends in mAb production processes. *Bioeng. Transl. Med.* **2**, 58–69 (2017).
4. Gottschalk, U. Bioseparation in antibody manufacturing: The good, the bad and the ugly. *Biotechnol. Prog.* **24**, 496–503 (2008).
5. Elgundi, Z., Reslan, M., Cruz, E., Sifniotis, V. & Kayser, V. The state-of-play and future of antibody therapeutics. *Adv. Drug Deliv. Rev.* **122**, 2–19 (2017).

6. O'Kennedy, R., Murphy, C. & Devine, T. Technology advancements in antibody purification. *Antibody Technol. J.* **6**, 17–32 (2016).
7. Giese, G., Myrold, A., Gorrell, J. & Persson, J. Purification of antibodies by precipitating impurities using Polyethylene Glycol to enable a two chromatography step process. *J. Chromatogr., B: Anal. Technol. Biomed. Life Sci.* **938**, 14–21 (2013).
8. Yang, H., Peczulis, P., Inguva, P., Li, X. & Heng, J. Y. Y. Continuous protein crystallisation platform and process: Case of lysozyme. *Chem. Eng. Res. Des.* **136**, 529–535 (2018).
9. Chew, K. W., Chia, S. R., Lee, S. Y., Zhu, L. & Show, P. L. Enhanced microalgal protein extraction and purification using sustainable microwave-assisted multiphase partitioning technique. *Chem. Eng. J.* **367**, 1–8 (2019).
10. Saxena, A., Tripathi, B. P., Kumar, M. & Shahi, V. K. Membrane-based techniques for the separation and purification of proteins: An overview. *Adv. Coll. Interface. Sci.* **145**, 1–22 (2009).
11. Szewczuk-Karpisz, K., Wiśniewska, M., Nowicki, P. & Oleszczuk, P. Influence of protein internal stability on its removal mechanism from aqueous solutions using eco-friendly horsetail herb-based engineered biochar. *Chem. Eng. J.* **388**, 156 (2020).
12. Wilson, J., Ristic, M., Kirkwood, J., Hargreaves, D. & Newman, J. Predicting the effect of chemical factors on the pH of crystallization trials. *Iscience* **23**, 101219 (2020).
13. Brange, J. & Vølund, A. Insulin analogs with improved pharmacokinetic profiles. *Adv. Drug Deliv. Rev.* **35**, 307–335 (1999).
14. Yang, M. X. *et al.* Crystalline monoclonal antibodies for subcutaneous delivery. *Proc. Natl. Acad. Sci. USA* **100**, 6934–6939 (2003).
15. Shenoy, B., Wang, Y., Shan, W. & Margolin, A. L. Stability of crystalline proteins. *Biotechnol. Bioeng.* **73**, 358–369 (2001).
16. Liu, H. F., Ma, J., Winter, C., & Bayer, R. Recovery and purification process development for monoclonal antibody production. *mAbs* **2**, 480–499 (2010).
17. Hebel, D., Huber, S., Stanislawski, B. & Hekmat, D. Stirred batch crystallization of a therapeutic antibody fragment. *J. Biotechnol.* **166**, 206–211 (2013).
18. Chen, W., Yang, H. & Heng, J. Y. Y. Continuous protein crystallization. in The handbook of continuous crystallization 372–392 (2020).
19. McPherson, A. & Shlichta, P. Heterogeneous and epitaxial nucleation of protein crystals on mineral surfaces. *Science* **239**, 385–387 (1988).
20. Hodzhaoglu, F., Kurniawan, F., Mirsky, V. & Nanev, C. Gold nanoparticles induce protein crystallization. *Cryst. Res. Technol.* **43**, 588–593 (2008).
21. Curcio, E., Fontananova, E., Di Profio, G. & Drioli, E. Influence of the structural properties of poly(vinylidene fluoride) membranes on the heterogeneous nucleation rate of protein crystals. *J. Phys. Chem. B* **110**, 12438–12445 (2006).
22. Georgieva, D. G., Kuil, M. E., Oosterkamp, T. H., Zandbergen, H. W. & Abrahams, J. P. Heterogeneous nucleation of three-dimensional protein nanocrystals. *Acta Crystallogr. D Biol. Crystallogr.* **63**, 564–570 (2007).
23. Sugahara, M., Asada, Y., Morikawa, Y., Kageyama, Y. & Kunishima, N. Nucleant-mediated protein crystallization with the application of microporous synthetic zeolites. *Acta Crystallogr. D Biol. Crystallogr.* **64**, 686–695 (2008).
24. Sengupta Ghatak, A. & Ghatak, A. Disordered nanowrinkle substrates for inducing crystallization over a wide range of concentration of protein and precipitant. *Langmuir* **29**, 4373–4380 (2013).
25. Hemming, S. A. *et al.* The mechanism of protein crystal growth from lipid layers. *J. Mol. Biol.* **246**, 308–316 (1995).
26. Ino, K. *et al.* Heterogeneous nucleation of protein crystals on fluorinated layered silicate. *PLoS ONE* **6**, e22582 (2011).
27. Hekmat, D., Huber, M., Lohse, C., Von Den Eichen, N. & Weuster-Botz, D. Continuous crystallization of proteins in a stirred classified product removal tank with a tubular reactor in bypass. *Cryst. Growth Des.* **17**, 4162–4169 (2017).
28. Lazo-Vélez, M. A., Serna-Saldívar, S. O., Rosales-Medina, M. F., Tinoco-Alvear, M. & Briones-García, M. Application of Saccharomyces cerevisiae var. boulardii in food processing: A review. *J. Appl. Microbiol.* **125**, 943–951 (2018).
29. Chen, H. *et al.* High production of valencene in Saccharomyces cerevisiae through metabolic engineering. *Microb. Cell Fact.* **18**, 1–14 (2019).
30. Faria, C., Borges, N., Rocha, I. & Santos, H. Production of mannosylglycerate in Saccharomyces cerevisiae by metabolic engineering and bioprocess optimization. *Microb. Cell Fact.* **17**, 1–11 (2018).
31. Lipke, P. N. & Ovalle, R. Cell wall architecture in yeast: New structure and new challenges. *J. Bacteriol.* **180**, 3735–3740 (1998).
32. Klis, F. M., Mol, P., Hellingwerf, K. & Brul, S. Dynamics of cell wall structure in Saccharomyces cerevisiae. *FEMS Microbiol. Rev.* **26**, 239–256 (2002).
33. Lesage, G. & Bussey, H. Cell wall assembly in Saccharomyces cerevisiae. *Microbiol. Mol. Biol. Rev.* **70**, 317–343 (2006).
34. Silvetti, T., Morandi, S., Hintersteiner, M. & Brasca, M. Use of hen egg white lysozyme in the food industry. in Egg innovations and strategies for improvements 233–242 (Elsevier, 2017).
35. Maia, N. J. L., Corrêa, J. A. F., Rigotti, R. T., Silva, A. A. & Luciano, F. B. Combination of natural antimicrobials for contamination control in ethanol production. *World J. Microbiol. Biotechnol.* **35**, 1–9 (2019).
36. Carrillo, W., García-Ruiz, A., Recio, I. & Moreno-Arribas, M. V. Antibacterial activity of hen egg white lysozyme modified by heat and enzymatic treatments against oenological lactic acid bacteria and acetic acid bacteria. *J. Food Prot.* **77**, 1732–1739 (2014).
37. Costa, V., Reis, E., Quintanilha, A. & Moradasferreira, P. Acquisition of ethanol tolerance in Saccharomyces cerevisiae: The key role of the mitochondrial superoxide dismutase. *Arch. Biochem. Biophys.* **300**, 608–614 (1993).
38. Lewis, J. G., Learmonth, R. P. & Watson, K. Induction of heat, freezing and salt tolerance by heat and salt shock in Saccharomyces cerevisiae. *Microbiology* **141**, 687–694 (1995).
39. Stahl, G., Salem, S. N., Chen, L., Zhao, B. & Farabaugh, P. J. Translational accuracy during exponential, postdiauxic, and stationary growth phases in Saccharomyces cerevisiae. *Eukaryot. Cell* **3**, 331–338 (2004).
40. Chayen, N. E. Turning protein crystallisation from an art into a science. *Curr. Opin. Struct. Biol.* **14**, 577–583 (2004).
41. McPherson, A. Crystallization of biological macromolecules. (1999).
42. Liang, M. *et al.* Cross-linked lysozyme crystal templated synthesis of Au nanoparticles as high-performance recyclable catalysts. *Nanotechnology* **24**, 245601 (2013).
43. Wei, H. *et al.* Time-dependent, protein-directed growth of gold nanoparticles within a single crystal of lysozyme. *Nat. Nanotechnol.* **6**, 93–97 (2011).
44. Wang, W. & Roberts, C. J. Protein aggregation–mechanisms, detection, and control. *Int. J. Pharm.* **550**, 251–268 (2018).
45. Wolstenholme, C. H. *et al.* Aggfluor: fluorogenic toolbox enables direct visualization of the multi-step protein aggregation process in live cells. *J. Am. Chem. Soc.* **142**, 17515–17523 (2020).
46. Sheinerman, F. B., Norel, R. & Honig, B. Electrostatic aspects of protein–protein interactions. *Curr. Opin. Struct. Biol.* **10**, 153–159 (2000).
47. Zhou, H.-X. & Pang, X. Electrostatic interactions in protein structure, folding, binding, and condensation. *Chem. Rev.* **118**, 1691–1741 (2018).
48. Smith, G. R. & Sternberg, M. J. E. Prediction of protein–protein interactions by docking methods. *Curr. Opin. Struct. Biol.* **12**, 28–35 (2002).
49. Zheng, X. Y., Shen, Y. H., Wang, X. Y. & Wang, T. S. Effect of pH on uranium (VI) biosorption and biomineralization by Saccharomyces cerevisiae. *Chemosphere* **203**, 109–116 (2018).
50. Nascimento, J. M., Oliveira, J. D., Rizzo, A. C. L. & Leite, S. G. F. (2019) Biosorption Cu (II) by the yeast Saccharomyces cerevisiae. *Biotechnol. Rep.* **21**, e00315 (2019).

Author contributions

M.B. performed most experiments, H.Y. and J.H. design the experiments and wrote the manuscript, X.M., W.W. performed some experiments. All authors reviewed the manuscript.

Funding

This article was funded by Engineering and Physical Sciences Research Council (Grant no. EP/T005378/1), Jilin Province Agricultural Science and Technology Innovation Project (Grant no. CXGC202102GH) and Science and Technology Development Plan of Jilin Province (Grant no. 20200301027RQ).

Competing interests

The authors declare no competing interests.

Additional information

Supplementary Information The online version contains supplementary material available at https://doi.org/10.1038/s41598-022-06999-7.

Correspondence and requests for materials should be addressed to H.Y. or J.W.

Reprints and permissions information is available at www.nature.com/reprints.

Publisher's note Springer Nature remains neutral with regard to jurisdictional claims in published maps and institutional affiliations.